JOURNAL OF GEOPHYSICAL RESEARCH, VOL. 91, NO. B6, PAGES 6305-6320, MAY 10, 1986

NATURE OF THE EASTERN BOUNDARY OF THE RIO GRANDE RIFT FROM COCORP SURVEYS IN THE ALBUQUERQUE BASIN, NEW MEXICO

Beatrice de Voogd, Larry D. Brown, and Carlene Merey

Institute for the Study of the Continents and Department of Geological Sciences
Cornell University, Ithaca, New York

Abstract. Reprocessing and synthetic seismic modeling of COCORP profiles across the eastern margin of the Rio Grande rift at Abo Pass, New Mexico, suggest that synthetic and antithetic Cenozoic normal faults sole into or are truncated by a northwest dipping listric master fault which bounds the eastern side of the basin and reaches a depth of at least 10 km beneath the southern Albuquerque basin. This fault appears to project toward the surface position of the Los Pinos Cenozoic normal fault, which lies basinward of and trends parallel to a mapped Laramide duplex thrust zone. The Los Pinos fault may sole into the older thrust, reactivating this preexisting compressional structure at depth. A lateral change in reflection amplitude and frequency is conspicuous across the eastern rift margin. Analysis demonstrates that source coupling is the main cause of a much deteriorated signal below the rift basin, although complex ray paths and attenuation by the graben fill may contribute.

Introduction

In 1975-1976 the Consortium for Continental Reflection Profiling (COCORP) collected 155 km of deep seismic reflection data both transverse and parallel to the axis of the Rio Grande rift (RGR) in the southern Albuquerque basin [Oliver and Kaufman, 1976; Brown et al., 1979]. Lines 1 and 1A (Figure 1) constitute an east-west transect across the central Albuquerque-Belen basin. Line 1, the focus of this analysis, begins on the faulted Cenozoic basin fill and ends to the east in the Los Pinos mountains. Cross line 2 provides some three-dimensional control on the fault geometry in the eastern part of the basin. Data acquisition and the initial processing was carried out by Petty Ray Geophysical Company. Those acquisition parameters and contractor processing sequence are described by Brown et al. [1980].

This paper focuses on major issues not fully addressed by previous studies and which include the possibility of a master fault underlying the Cenozoic normal faults, the role of Laramide and older structures in the rift evolution, the three-dimensional geometry of normal faults, and the cause of dramatic changes in reflection amplitudes and frequencies across the eastern rift boundary. Reprocessing and reanalysis of lines 1 and 2, together with synthetic seismic modeling, provide substantial new insight into these issues. Three-dimensional aspects of the data are quantitatively discussed in interpreting fault geometry.

Paper number 5B5517.
0148-0227/86/005B-5517$05.00

Major findings of the New Mexico COCORP surveys have been reported by Brown et al. [1979, 1980]. The most striking result is an unusually strong midcrustal reflector which is believed to be a tabular magma body previously inferred from unusually strong shear waves reflections noted in microearthquake studies in the Socorro region [Sanford et al., 1973; Brocher, 1981b]. Brown et al. [1980] suggested that closely spaced high angle normal faults might be responsible for the structural relief observed on the floor of the Albuquerque basin. Cape et al. [1983], however, interpreted migrated versions of the COCORP sections to indicate that the Cenozoic faults flatten within the upper 5 or 6 km of the crust. The above studies have failed to trace faults beneath a few kilometers depth, raising questions about the style of extension beneath the sedimentary section.

In the new structural interpretation presented herein, shallow Cenozoic faults sole into or are truncated by a relatively continuous reflector which is thus interpreted as a Cenozoic fault surface. To the east, this master fault may coincide at the surface with the Los Pinos normal fault, which is the boundary between the Albuquerque basin and the Los Pinos-Manzano mountain range. The Los Pinos fault is basinward from and parallel to the Paloma and Montosa faults (Figure 1), which are mapped as Laramide thrusts [Stark and Dapples, 1946; Kelley, 1977]. The spatial correlation between late Cenozoic fault scarps and Laramide thrusts along the east side of the rift may indicate reactivation at depth of older compressional structures [Kelley, 1977].

Reflections from beneath the basin have lower frequencies and are much weaker than those under the eastern flank. These differences in amplitude and frequency content are correlated with changes in the surface geology and are shown to be due mainly to variations in coupling of the vibrators to the ground. Further signal degradation may also have resulted from selective loss of the high frequencies within the graben fill by seismic attenuation and imaging difficulties associated with ray path distortion through the structurally disrupted sedimentary section. Thus the lateral change in seismic character observed across the rift boundary does not represent structural or compositional variations at depth but is due to the masking effects of near-surface seismic phenomena. A near-vertical blank zone extending vertically downward from the eastern edge of the basin appears to be an artifact due to improper stacking of common midpoint (CMP) data across an area of large lateral velocity variations rather than being representative of some deeply penetrating geological structure, e.g., intrusion or fault zone, as previously speculated [Brown et al., 1980].

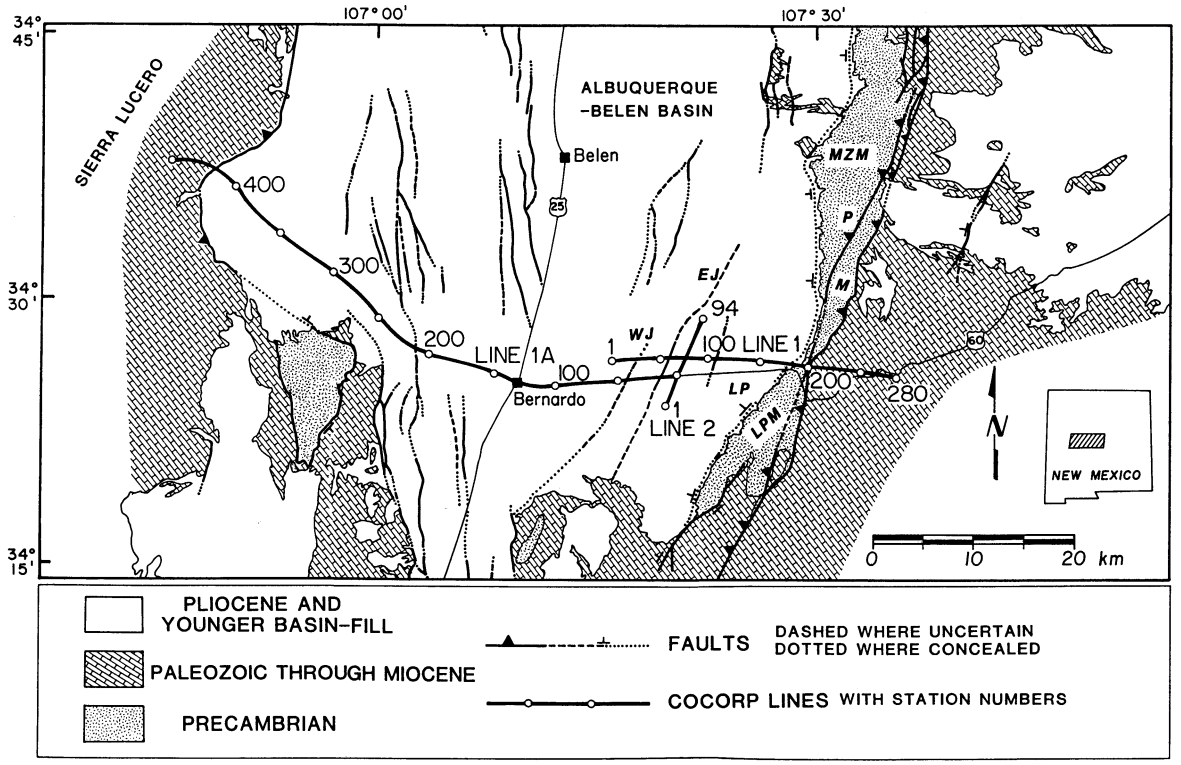

Fig. 1. Location map; geology sketched from Kelley [1977], Machette [1978, 1982], and Machette and McGimsey [1983]. MZM and LPM are the Manzano and Los Pinos mountains, respectively, which constitute the ranges bounding the southern Albuquerque basin to the east; LP is the Los Pinos normal fault; P and M are the Paloma and Montosa faults, interpreted as Laramide thrusts; WJ and EJ are two normal faults prominent on the COCORP sections and discussed in the text.

Background

The Albuquerque basin belongs to a series of en echelon north trending grabens or half grabens that form the Rio Grande depression, a late Cenozoic extensional feature superimposed upon a north trending tectonic belt deformed during late Paleozoic and again during the Laramide orogeny [Chapin, 1979]. The Albuquerque basin is an asymmetric graben, roughly 145 km long and 50 km wide, essentially filled by nonmarine Cenozoic deposits. Rifting in this area started at about 26 Ma, as suggested by the study of bolson sedimentation and age of volcanism [Chapin and Seager, 1975]. COCORP line 1 crosses the eastern side of the central graben at Abo Pass, a physiographic constriction between the Manzano and the Los Pinos mountains (Figure 1).

A set of layered and faulted strong reflectors defines the structural complexity of the rift basin (C in Figure 2). This sequence of shallow, correlatable reflectors, approximately 2 km thick, is interpreted as the Paleozoic-Mesozoic sedimentary section which outcrops south of line 2A [Brown et al., 1980] and east of Abo Pass. The base of C is believed to mark the top of the Precambrian basement. West of vibration point (VP) 180 (line 1), the structural relief observed on the seismic section corresponds to the Hubell-Joyita bench, which is buried under Quaternary fill in the vicinity of line 1 [Kelley, 1977]. On line 1, the syn-rift basin fill appears to reach a maximum thickness of about 2500 m at VP 80. This basin fill mainly consists of Miocene-Pliocene gravels, arkose, and tuffs of the Santa Fe Group, commonly covered by Quaternary alluvial sands and gravels [Foster, 1978]. A detailed discussion of the Cenozoic stratigraphy of the basin can be found in the work by Chapin and Seager [1975]. Although Jurdy and Brocher [1980] used sonic logs to correlate velocities determined from COCORP refracted arrivals with geological units, existing deep drill holes are too distant from the COCORP lines to provide stratigraphic control on specific reflecting horizons.

Both listric normal faulting and "domino style" planar normal faulting have been suggested from geological field studies in the Albuquerque basin [e.g., Woodward, 1977; and Chamberlin, 1983]. Line 1 intersects several normal faults which offset reflectors C (Figure 2) and have been interpreted as steeply dipping Cenozoic faults from geological mapping [Kelley, 1977]. The two east dipping normal faults which cross line 1 at VP 32 and VP 60 (Figure 1) are identified as the West and East Joyita faults (WJ, EJ), respectively, of Kelley [1977]. The Los Pinos normal fault (Figure 1) marks the eastern boundary of the main rift basin [Kelley, 1977].

In the Los Pinos mountains, between VPs 188 and 202, line 1 traverses several outcropping Precambrian units which have been thrust eastward against Pennsylvanian strata along two major

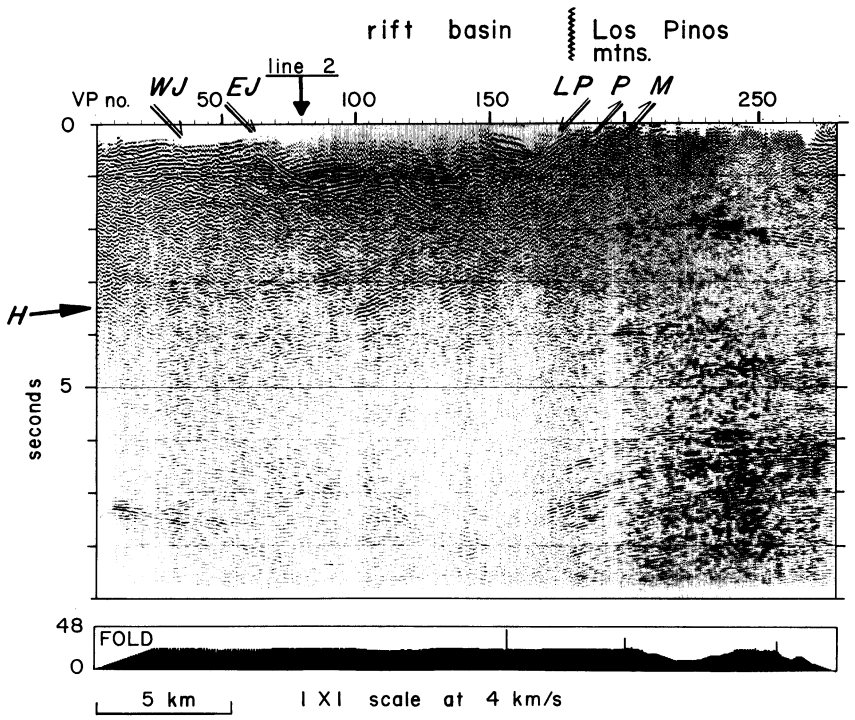

Fig. 2a. Reprocessed section from COCORP Abo Pass line 1; true amplitude relationship is preserved from trace to trace; amplitudes are not corrected for geometrical spreading using a velocity function, but a vertical exponential gain is applied for display purpose.

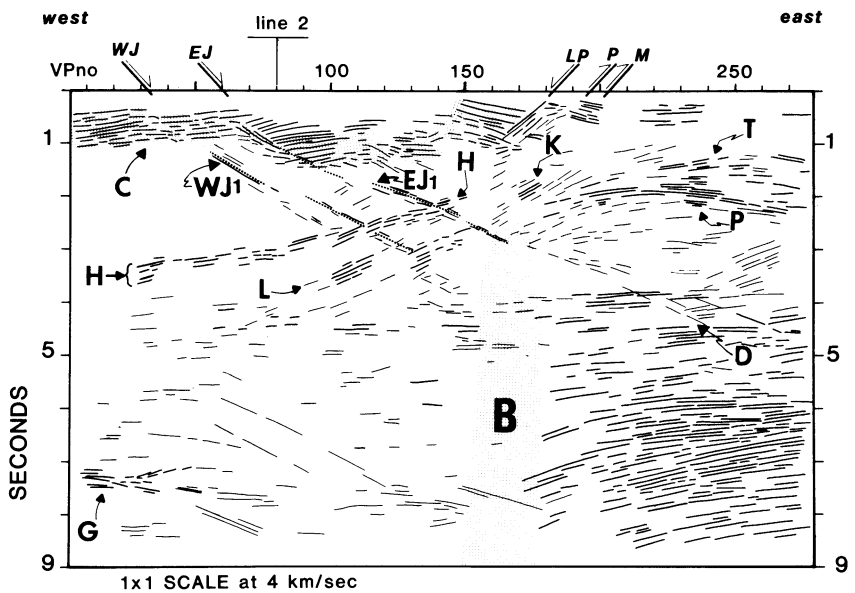

Fig. 2b. Interpretive and schematic line drawings of COCORP Abo Pass line 1 (Figures 2a and 9); as determined from the COCORP data, east dipping normal faults reach the surface at VPs 32, 60, 100, 109, and west dipping faults at VPs 120, 145, 150; only faults discussed in the text are labeled (WJ, EJ, LP, P, M). Dashed lines underline reflections from the Joyita fault planes. The inferred Paleozoic-Mesozoic section (labeled C) is shaded, as well as a near-vertical zone apparently devoid of continuous reflections (B); G is inferred to represent the edge of a midcrustal magma chamber [Brown et al., 1979]; other events labeled are discussed in text.

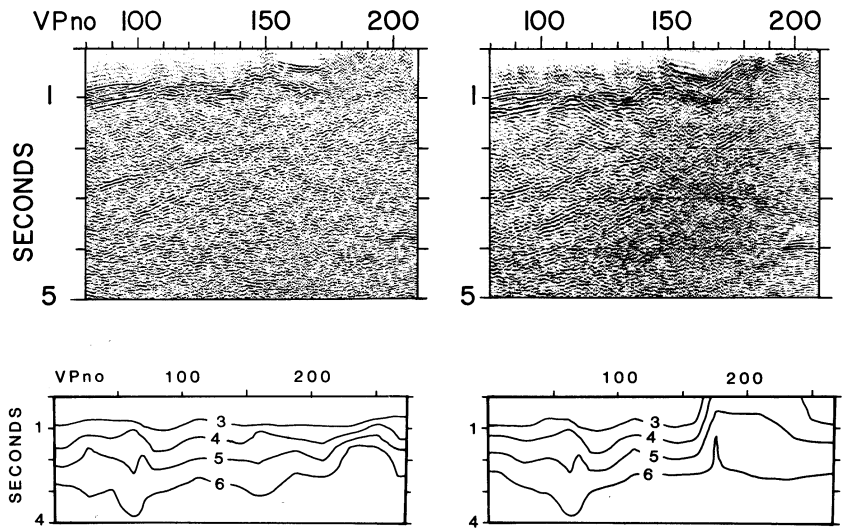

Fig. 3. Comparison between the initial contractor processing (left) and our reprocessing (right); top is a detail of COCORP line 1; key reflections (such as H, L, and EJ1, labeled on figure 2) are identifiable in both versions; both sections are displayed with the same automatic gain control; bottom part shows the stacking velocities (rms) used to produce the sections above, contoured every kilometer per second.

faults, the Montosa and the Paloma thrusts. These thrusts strike roughly N-NE, have near-surface dips of 40°-50° and a vertical offset of at least 700 m [Stark and Dapples, 1946; Reiche, 1949]. This fault movement has been inferred to correlate with similar movements in the Southern Rocky mountains during the Laramide orogeny (90-50 Ma) [Stark, 1956; Kelley, 1977]. Interpretation of previous versions of the COCORP data have failed to unambiguously relate particular reflections with these faults. Brown et al. [1980] suggest that perhaps events H or L (Figure 2) may represent the subsurface expression of the Montosa or Paloma thrust, a possibility more fully addressed here.

Numerous seismic events are observed down to approximately 12 s (35 km) throughout the whole body of the New Mexico COCORP surveys. The depth to Moho of 33-38 km inferred from wide-angle experiments [Toppozada and Sanford, 1976; Olsen et al., 1979] corresponds to travel times between 11 and 13 s on the COCORP profiles. Prominent reflections in this depth range are observed on the COCORP sections, especially beneath the rift flank on line 1 and within the central graben on line 2A [Brown et al., 1980], and presumably represent the crust-mantle transition. As imaging of these lower crustal events has not been significantly improved by our reprocessing and we have little to add to previous interpretations in this regard, we focus on upper crustal structures, and the seismic sections are displayed only from 0 to 9 s (about 26 km).

Reprocessing

The main goal of the reprocessing was to better image reflections from within the basement below the rift basin. This reprocessing was carried out on COCORP's MEGASEIS (T.M. Seiscom Delta) computer system. Improvement in the stacked section of line 1 (Figure 3) was obtained primarily by careful velocity analysis and lateral prestack amplitude balancing. Higher stacking velocities were used to enhance dipping events such as EJ1, H, and L (Figure 2) and discriminate against subhorizontal multiples from the rift basin. It is a common practice to balance trace amplitudes before stack. Here, true amplitude relationships from trace to trace were preserved by applying surface-consistent amplitude corrections calculated from the unstacked data. This process corrects for those components of the amplitude that are unrelated to the subsurface.

Frequency-wave number (FK) analysis of some of the field records indicate that backscattering of the seismic signal could be a source of noise. However, two-dimensional (pie slice) filtering did not significantly improve the seismic section. Other processing steps were not significantly changed from the initial contractor processing (Table 1) since they were deemed adequate. Detailed refraction statics corrections could possibly improve the sections. However, such analysis is hindered by the large near offset (600 m). Although some improvements were obtained by this more extensive reprocessing, key reflections are identifiable in both the old and new versions (Figure 3). The interpretation discussed here results more from a new and more critical look at these data, paying particular attention to possible artifacts such as near-surface effects and side swipe than to previously overlooked or erroneous aspect of processing.

Although the reprocessing reported here was extensive (see Table 1), it by no mean exhausted what might potentially be done. For example, numerous crossing events of various dips are seen below the rift basin (Figure 2). Since the conventional CMP stacking tends to filter on the basis of dip, further improvement of the seismic section might require prestack partial migration and dip moveout [Hale, 1984]. Additional difficulties come from three-dimensional and velocity

TABLE 1. Data Processing (Following Demultiplex and Vibroseis Correlation)

Initial Contractor Processing	Cornell Reprocessing (This Paper)	
	To Produce Section in Figure 2	Others
1, trace editing	1, trace editing	deconvolution
2, deconvolution (operator of 320 ms, prediction lag of 48 ms)	2, statics corrections	F-K filtering
3, brute stack	3, velocity analysis (Figure 3)	automatic residual statics
4, refraction study (field statics)	4, mutes before and after dynamic corrections	range stacks
5, velocity analysis	5, partial correction for spherical divergence using a vertical exponential gain, and lateral amplitude balancing	Kirchoff migration
6, CMP sort		
7, mutes and final dynamic corrections		
8, automatic residual statics		
9, stack, film display	6, stack, display	

The source consisted of five vibrators generating a 10-32 Hz linear sweep.

pull-down effects. Because the COCORP lines often run at an angle of 60° or less to the strike of the structures imaged, three-dimensional aspects of the data must be considered or side swipe will not be properly migrated. Two-dimensionally migrated seismic sections cannot be treated as geologic cross sections when calculating the true dip of a structure (Figure 4). Fault planes, for example, may appear more listric than they really are. Three-dimensional factors were, in fact, found to be significant in this analysis.

Large lateral changes in velocity corresponding to the variation in thickness of the basin fill undoubtedly cause complex velocity pull-down effects and ray path distortions that cannot be handled by conventional time migration schemes [Peddy et al., 1986; Larner et al., 1981]. Furthermore, CMP smearing associated with these complex structures will not be corrected by poststack migration.

Although advanced capabilities such as prestack migration were not available on the MEGASEIS, synthetic seismic modeling was available to constrain the interpretation with respect to the above problems. Synthetic seismic sections were computed with the AIMS modeling package (TM Geoquest International). Even though AIMS is formally two-dimensional, three-dimensional effects are discussed in the following analysis.

Shallow Fault Geometry

Intrarift Cenozoic faulting is evident from conspicuous offsets of Phanerozoic strata on line 1 (events C, Figure 2). Because they project upwards toward faults identified on the basis of basin fill truncation and/or surface geology, a few weak, dipping events in the upper 3 s of the seismic section from line 1 are interpreted as fault plane reflections (e.g., EJ, WJ Figures 2b and 5). On the seismic section of line 1, these inferred fault plane reflections have fairly low apparent dip (less than 20°). When correlated with overlying offsets in the Paleozoic-Mesozoic section (C, Figure 2b), these low dips suggest listric fault geometry. Cape et al. [1983] interpreted the Joyita faults to be listric, flattening in the upper 5 km and in particular "recognized listric faulting in the subsurface by the seismic expression of the East Joyita fault." However, line 1 runs at an angle of 60° to the average strike of the Joyita faults where these are mapped. As we shall show, proper consideration of three-dimensional effects leads to different conclusions.

Cross line 2 provides some constraints on three-dimensional fault geometry. Line 2 is roughly parallel to the Joyita faults as mapped at the surface (Figure 1); thus reflected arrivals from these fault planes should give horizontal events on the seismic section from line 2 if their strike does not change with depth. There is a weak horizontal reflection at 2 s (about 5 km) on line 2 (WJ2, Figure 5), which is more clearly seen on the constant velocity stack displayed in Figure 6. This reflection ties with dipping reflections associated with the West Joyita fault on line 1 (WJ1, Figures 2 and 5). It is conceivable that WJ2 could be a side reflection from the East Joyita fault scarp, corresponding to a ray traveling in the shallow low-velocity layer (less than 2.8 km/s). However, velocity analysis yields a stacking velocity of 4.6 km/s for event WJ2 (line 2), consistent with its being from a deeper portion of the West Joyita fault plane rather than a surficial arrival.

Reflections WJ1 and WJ2 give us the true dip and strike of the West Joyita fault at the intersection of lines 1 and 2. Assuming a velocity between 4.5 and 6 km/s along reflector WJ1, the true dip of the West Joyita fault, as determined from the relation in Figure 4, is 51° (+/-4°) at a depth of about 5 km. The surface location of the West Joyita fault is constrained by offsets in first arrivals to lie between VPs 31 and 33 of line 1 (Figure 7a). Reasonable fault plane geometries that are consistent both with the known surface location of the West Joyita fault and with its true dip (about 51°) calculated at the intersection of lines 1 and 2 are drawn in Figure 7b. The above analysis indicates that the West Joyita fault is a northeast striking structure that might be planar or slightly listric, in that latter case having a surface dip of about 55°, flattening to only 47° in the upper 5 km (Figure

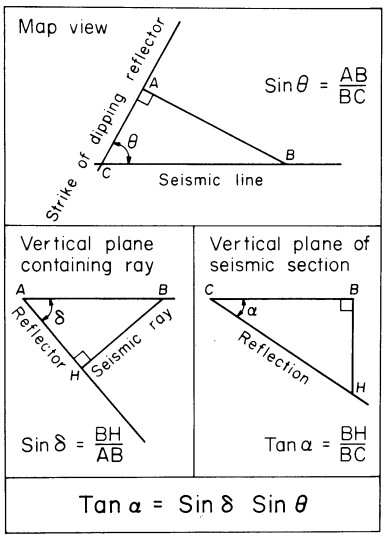

Fig. 4a. Migration and strike-dip correction for side reflections from a dipping plane; the dipping reflective surface and the seismic section are treated as planes (locally a reasonable approximation); seismic rays are approximated by straight lines (homogeneous medium); θ is the angle between the strike of dipping surface and the seismic line (55° between the West Joyita fault and line 1); δ is the true dip of the dipping surface, measured from the horizontal; α is the apparent dip measured on the seismic section (before migration); if the strike of the dipping structure is unknown, the true dip and strike can be calculated if the reflector is imaged on an additional seismic line (index 2) nonparallel to the first seismic line (index 1): $\sin\delta = \tan\alpha_1/\sin\theta_1 = \tan\alpha_2/\sin\theta_2$, and $\theta_1 + \theta_2 + \beta = 180°$ give $\tan\theta_1 = \sin\beta/[(\tan\alpha_2/\tan\alpha_1) + \cos\beta]$.

7b). This conclusion is further supported by the synthetic modeling discussed in the next section. Note that if line 1 were treated in a two-dimensional fashion, the 33° apparent dip of the West Joyita fault plane reflection (WJ1, Figure 2) would "migrate" to a dip of 40°. If such a two-dimensionally migrated section were treated as a geologic cross section, after correction for strike using the relation between apparent and true dip derived for geologic cross section [e.g., Ragan, 1973, pp. 1-6] (Figure 4b), an erroneous "true" dip of 43° would be found.

According to Figure 5, reflections from the East Joyita fault plane should arrive at about 1.2 s on line 2. A series of north dipping reflectors (R in Figure 5) represent the synrift sequence on line 2, yielding a true dip of 10°-15° to the northwest. Underlying the basin fill R, two sets of strong and continuous dipping events (C2 and EJ2, Figure 5) cross each other below VP 80 (line 2). The north dipping package C2 ties with sequence C on line 1. EJ2 is somewhat more planar and less cyclic than C2. If C2 is the Mesozoic-Paleozoic sequence (C on line 1), EJ2 is reasonably identified as the East Joyita fault plane reflection. The apparently poor tie between reflections EJ1 and EJ2 seen on Figure 5 may be due to three-dimensional effects. Several authors indicate a change in the strike of the East Joyita fault in the vicinity of line 2 [Kelley, 1977; Machette, 1978]. Reflections from the East Joyita fault cannot be recognized on the southern part of line 2 probably because such events would arrive at 1-1.2 s and thus be hidden by sequence C. If in its northern portion line 2 runs closer to the East Joyita fault (Figure 1), side reflections from the East Joyita fault plane will appear earlier and possibly before C2. This happens around VP 70 where event EJ2 starts arriving before C2. Thus the apparent dip of the inferred East Joyita fault reflection on line 2 may reflect its convergence with the northern end of line 2 (Figure 1); alternatively, EJ2 could represent a tilted block of Mesozoic-Paleozoic strata obscuring a possible reflection from the East Joyita fault.

Reflections both from the West and East Joyita fault planes (WJ1, EJ1, Figure 2) can be traced to a depth of about 6 and 7 km, respectively, where these faults appear to cross a relatively continuous horizon (H, Figure 2). At that depth, these faults have true dips of at least

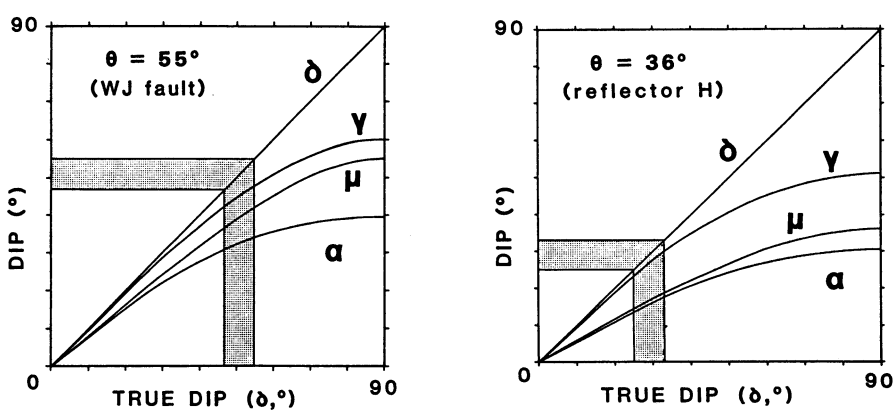

Fig. 4b. Summarizes how side swipe affect dips on a seismic section; μ is the two-dimensionally migrated dip ($\sin\mu = \tan\alpha$); after correction using relation between apparent and true dip of geologic cross section, the dip is γ, related to μ by $\tan\mu = \tan\gamma \sin\theta$; the shaded areas correspond to the values of interest for reflector WJ and H, respectively; note that a two-dimensionally migrated seismic section cannot be treated as a geological cross section.

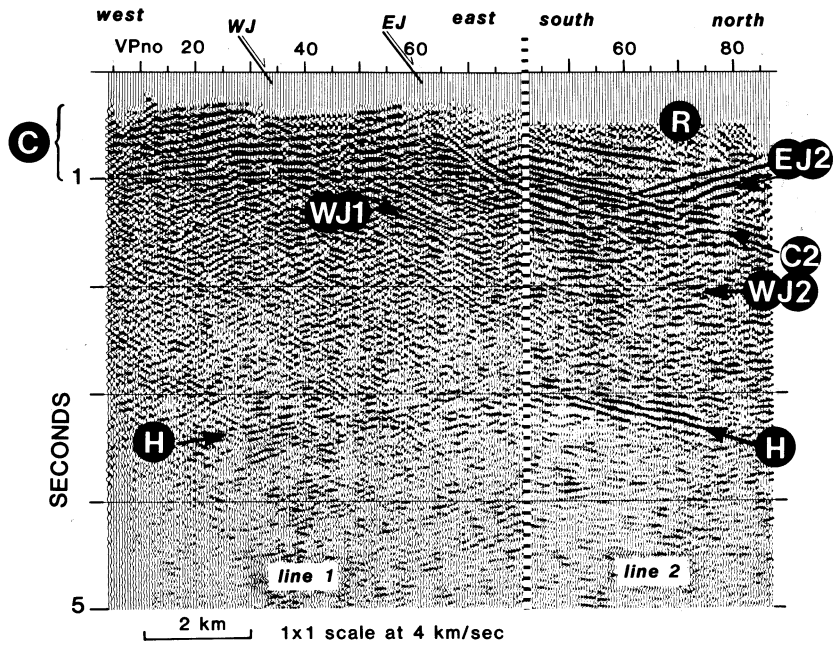

Fig. 5. The western portion of line 1 (to the left) is tied with the northern portion of line 2 (to the right); events WJ1 and WJ2 are interpreted as reflections from the West Joyita fault (WJ) that strikes almost parallel to line 2; reflection H dips to the northwest; package C2 is inferred to represent the Mesozoic-Paleozoic sequence on line 2, tying with series of reflections C on line 1; R represents the low-velocity graben fill; EJ2 may be a side reflection from the East Joyita fault scarp.

30°, indicating that the Joyita faults are not as listric as suggested by Cape et al. [1983], who infer that they become essentially flat within 5 km depth. The West Joyita fault can be shown to be planar or close to planar in the vicinity of the COCORP survey, whereas the amount of curvature of the East Joyita fault cannot be determined from these data alone. What happens to the Joyita faults at depths greater than 7 or 8 km (about 3 s) is less clear, but some possibilities are discussed in the next section.

An Intrabasement Master Fault

Refracted arrivals (Figure 8) show offsets at VPs 182, 193, and 202 that are attributable to the Los Pinos, Paloma, and Montosa faults, respectively. Stacked sections including only

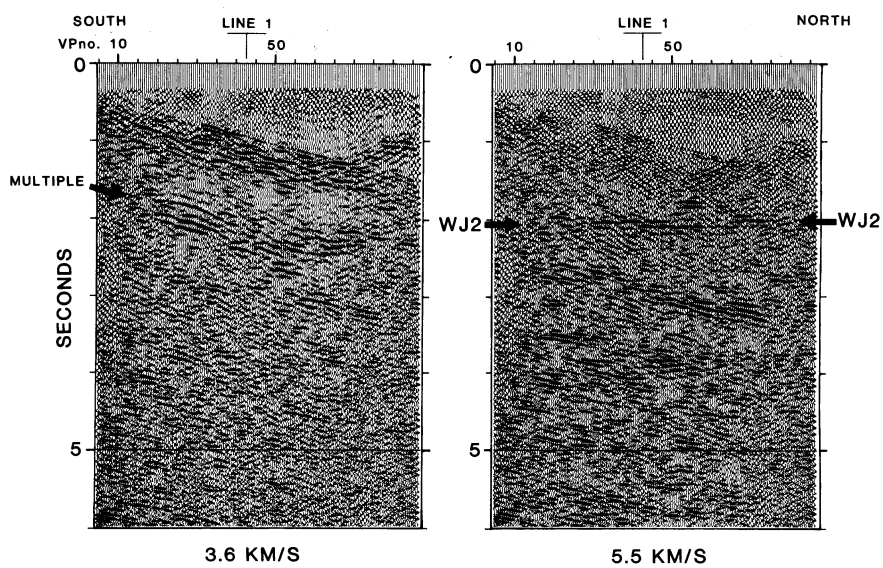

Fig. 6. Constant velocity stacks of Abo Pass line 2; the section to the right was stacked with a velocity (5.5 km/s) higher than the stacking velocity of event WJ2 (4.6 km/s) in order to further attenuate the inferred multiple shown on the left.

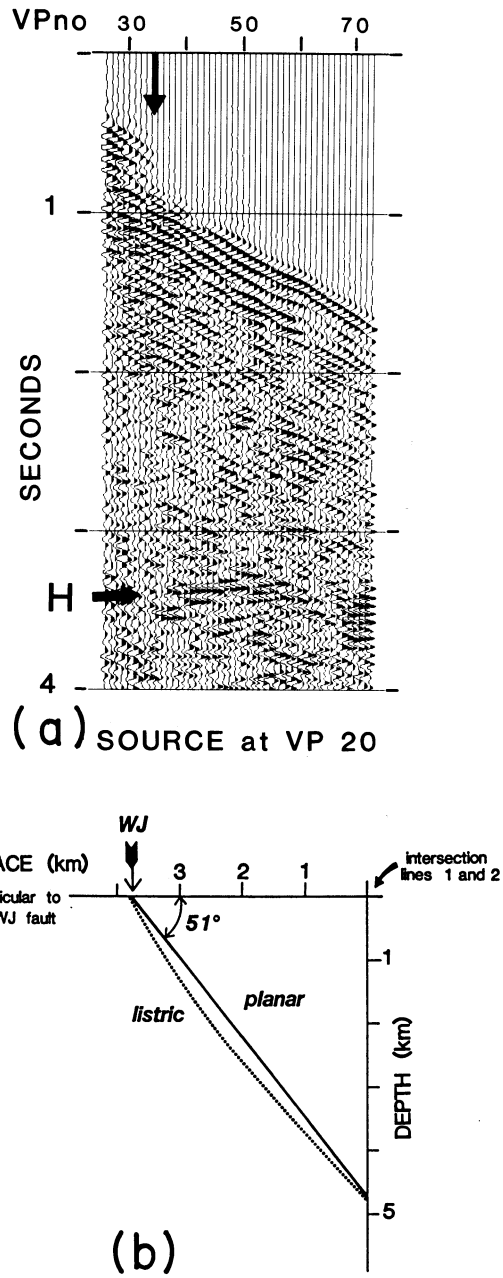

Fig. 7. Amount of curvature of the West Joyita fault plane.
(a) Shot point gather from line 1, showing the surface location of the West Joyita fault; the vertical arrow between VPs 34 and 35 points to the corresponding break in the arrival refracted at the interface between the 2.2 and 3.5 km/s layers; trace spacing is 100 m, with a near-offset of 600 m; from this record, and in agreement with adjacent shots, the depth to the 2.2-3.5 km/s interface is calculated to be 210 m; this constrains the surface position of the West Joyita fault to lie between VPs 31 and 33; note also a strong reflection at 3.4 s that corresponds to H (Figure 2).
(b) Geometries of the West Joyita fault plane permitted by our analysis; the dotted line indicates the maximum amount of curvature allowed.

source-receiver offsets of less than 2300 m seem to indicate the existence of weak west dipping events that might correspond to the shallow parts of the Paloma-Montosa fault zone (Figure 9), below the Los Pinos mountains.

Two distinct, though discontinuous, series of reflections can be traced below the rift basin between 2 and 4.5 s over a horizontal distance of about 18 km (labeled H and L, Figure 2). The surface projection of H and L is ambiguous; if dips beneath VPs 140-160 were extrapolated, these structures should project to the surface near VPs 200 and 230, respectively. Yet from geological mapping (M.N. Machette, written communication, 1984) as well as the COCORP section itself, there is little indication of west dipping structures in the near-surface east of the Montosa fault, aside from a small NE trending fault scarp east of the Manzano mountains (Figure 1) [Machette, 1978]. Both series of events H and L can be identified on cross line 2 (Figure 5) and thus can be shown to dip to the northwest. H strikes N49°E (+/-4°) and dips 29° (+/-4°) to the north west at a depth of 7 km where lines 1 and 2 intersect, assuming an average velocity of 6 km/s at that depth. This strike is significantly different from the overall trend of the Albuquerque basin and bordering uplifts (N20°E). However, it is quite consistent with the strike of the Los Pinos fault immediately south of the COCORP profiles (Figure 1).

H is a relatively strong series of reflection segments correlatable over a horizontal distance of 12 km, with an average stacking velocity of approximately 6 km/s. Its amplitude is highly variable, possibly because of focusing effects induced by the thick low velocity graben fill.

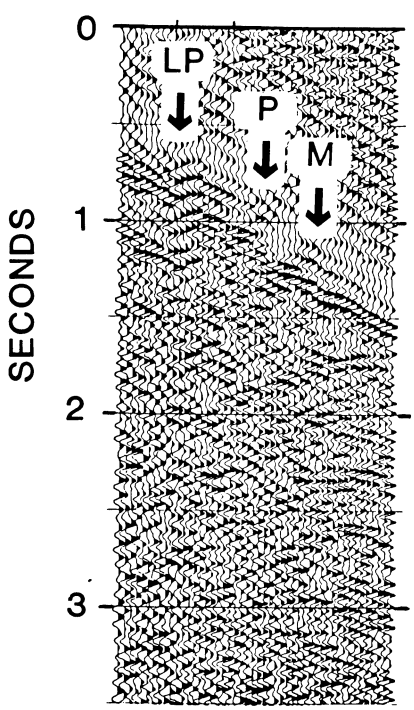

Fig. 8. Shot point gather for source at VP 160 showing the location of the Los Pinos, Paloma, and Montosa faults, labeled LP, P, and M, respectively.

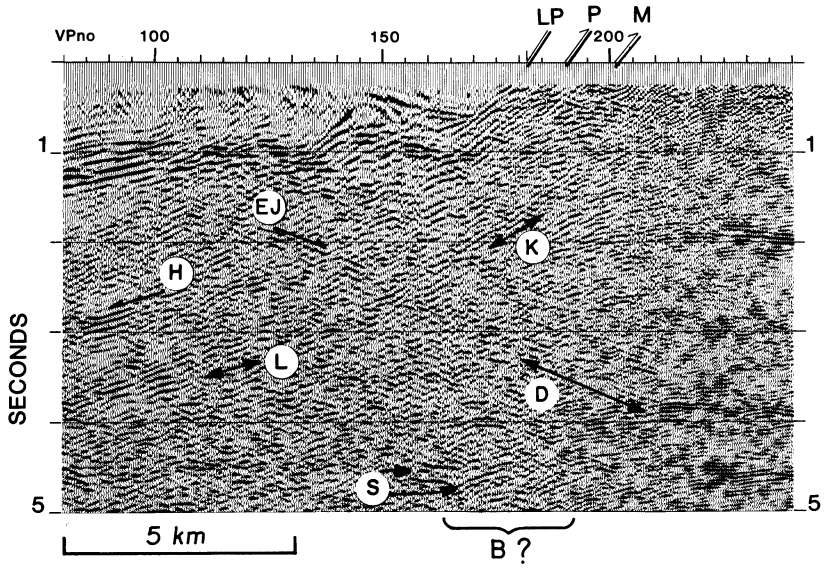

Fig. 9. Near-range stack of COCORP Abo Pass line 1; only traces with source to receiver spacing less than 2300 m were used to produce this section (average fold 10), otherwise processed like the section in Figure 2, except for automatic gain control (AGC) applied after stack for display purposes. Note west dipping event (labeled K) beneath VPs 160-200; after migration, this event projects to the surface at VP 230. Below VPs 160-180, a near-vertical zone apparently devoid of continuous reflections was conspicuous on previous versions of this section (Brown et al, [1980]; labeled B, Figure 2) but is not seen on this stack.

L, somewhat less continuous and less strong than H, also dips to the northwest but more steeply.

Reflections H and L lack continuity, appearing broken up in several places, which might initially lead to the conclusion that they represent prerift features subsequently disrupted during Cenozoic extension. However, because of large lateral velocity contrasts between basement rocks and basin fill, velocity pull-down effects and ray path deflection might also give a segmented appearance to reflectors H and L even if they were continuous horizons. Two-dimensional normal incidence ray tracing was used to evaluate this possibility.

A two-dimensional model was postulated from the thickness on the seismic section of the inferred Mesozoic-Paleozoic sequence (C, Figure 2) and the velocity estimates deduced by Brocher's [1981a] study of COCORP refracted arrivals. These velocities were chosen instead of interval velocities computed from stacking velocities, since small errors in stacking velocities can lead to large errors in interval velocities [Al-Chalabi, 1974]. The instability of such estimates is compounded by the structural complexity, e.g., various dips, encountered on line 1.

Zero-offset (single fold) synthetic seismic sections were used to quantitatively illustrate migration and velocity pull-down effects. Waveforms were not modeled. A 10-32 Hz Klauder wavelet was used to produce the synthetics. As discussed in the next section, the high-frequency part of the sweep is poorly generated in or transmitted through the basin fill. Therefore the seismic data have a somewhat broader wavelet than the synthetics. The synthetic section from our preferred model (Figure 10a) is shown superimposed on the actual seismic section (Figure 11) and can also be compared to the same section shown unmarked in Figure 2a.

The model in Figure 10a postulates that reflector H is continuous and truncates the Joyita fault planes. Yet its seismic image is segmented (Figures 11 and 12a). The apparent offsets in reflector H are due to velocity pulldown associated with varying thicknesses of graben fill. The severity of this pulldown is obvious from the disrupted reflection from the flat reference horizon (R, Figure 11b). As much as 400 ms of velocity pull-down can be expected when correlating events across the eastern side of the basin.

The model in Figure 10b assumes that the normal faults offset the deeper reflector H. The amount of offset across H is chosen equal to the observed offset of the prerift section on the seismic data (C, Figure 2). The seismic response of this model also shows a relatively complex reflection geometry (Figure 12b). Careful comparison of the synthetics in Figures 12a and 12b with the actual data (Figure 11) indicates that the first model is more likely, i.e., that the Joyita faults terminate into a continuous reflector. According to the second model, there should be a large offset in H beneath VPs 80 and 130 (areas circled in Figures 12a and 12b). The seismic section shows no such offset. Rather reflection H appears continuous like the synthetics in Figure 12a.

The model in Figure 10c postulates that the East Joyita fault truncates reflector H. In addition, a west dipping interface K is introduced such as to match reflection K observed below VPs 160-200 (Figures 2 and 9). This interpretation is further suggested by an event that appears to extend reflection EJ1 to the east (D, Figures 2

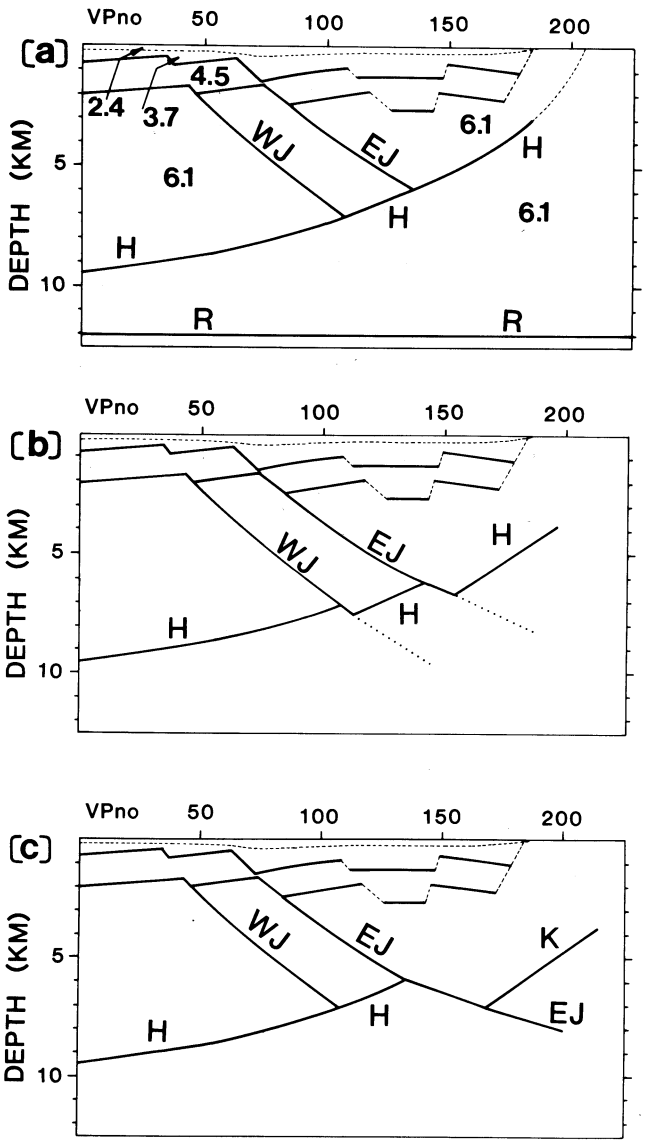

Fig. 10. Models for Abo Pass line 1 corresponding to synthetics shown in Figures 11 and 12; dotted lines represent horizons not shown in synthetics for clarity; however, rays were refracted across these interfaces as well. Velocities are taken from a study of COCORP refracted arrivals [Brocher, 1981a] and do not necessarily represent rock units. Velocities (km/sec) are indicated on model in Figure 10a. Small velocity contrasts (a few percent) were arbitrarily introduced to get reflections from the faults at depth. (a) Model in which the Joyita faults sole into or are truncated by a continuous reflector H; this model appears to provide a good fit to the data; a horizontal reference reflector (R) is added at the arbitrary depth of 12 km to illustrate velocity pull-down effects. (b) Model in which the Joyita faults disrupt the underlying reflector H postulated in Figure 10a; the amount of offset across H is chosen equal to the observed offset of the prerift section on the seismic data. (c) Model in which the East Joyita fault truncates H; interface K is located such as to match a fair west dipping reflection (K, Figures 2 and 9) observed below VP 180.

and 9); however, event D matches diffraction curves for about 6.2 km/s at 7 km depth, indicating that D is a diffraction, most likely from the intersection of the East Joyita fault and H as shown in the model of Figure 10a. Furthermore, modeling shows that D is in the wrong place to be an extension of the East Joyita fault plane (Figure 11). Thus reflections from the East Joyita fault plane are not seen eastward of VP 166 (Figure 12a). The model in Figure 10c and 12c also shows that reflection K is unlikely to correlate with H.

The above modeling demonstrates that time delays and ray path distortion due to near-surface structural complexity explain the segmented appearance of reflection H (Figure 2). Thus a relatively continuous horizon (H) may underlie the southeastern part of the Albuquerque basin. It seems to project to the east side of the basin in an area where both Cenozoic normal faults and Laramide thrusts are mapped.

If H is not substantially offset, if at all, by the overlying Cenozoic normal faults, as the modeling suggests, then any Cenozoic extensional faulting must be accommodated along H, above H, or H must be a younger feature. Thus three alternative explanations for H seem plausible: H is a Cenozoic normal fault, a Laramide thrust, or a Laramide thrust reactivated as a Cenozoic normal fault. The geometry implied by the first model above (Figure 10a) suggests that H may be either the deeper extension of the Los Pinos normal fault, into which the shallow faults of the Hubbell bench sole or truncate, or that H may be the extension of the Laramide fault system corresponding to the Paloma and Montosa faults. If the latter is correct, it implies that Cenozoic extension in this area follows older Laramide structures.

Modeling is consistent with L being a multiple of H, generated within the low-velocity basin fill. However, it is conceivable that L is a splay of the same fault system as H. Other weak west dipping events observed below VPs 160-210 (e.g., K, Figure 9) may also represent splays of this fault system. The multicyclic reflection character of H (and L) is similar in many respects to reflections observed from the Wind River thrust, a Laramide compressional feature in western Wyoming [Smithson et al., 1979], as well as to reflections associated with the Sevier Desert Detachment, a major extensional structure in west central Utah [Allmendinger et al., 1983]. The duplex zone mapped at the surface between VPs 190 and 206 [Myers, 1977; Myers et al., 1981] may continue at depth as a broad shear zone of interlaced lithology, giving rise to a layered reflection appearance. Synthetic seismic modeling shows that the laminated or anastomosing geometry of mylonites can produce prominent multicyclic reflections similar to those observed in deep seismic reflection profiles [Fountain et al., 1984]. However, the narrow bandwidth of the data (less than two octaves) precludes further discussion of reflection seismic character.

Change in Seismic Character Across the Eastern Rift Boundary

A dramatic lateral change in seismic character is observed around VP 188 on the seismic stacked

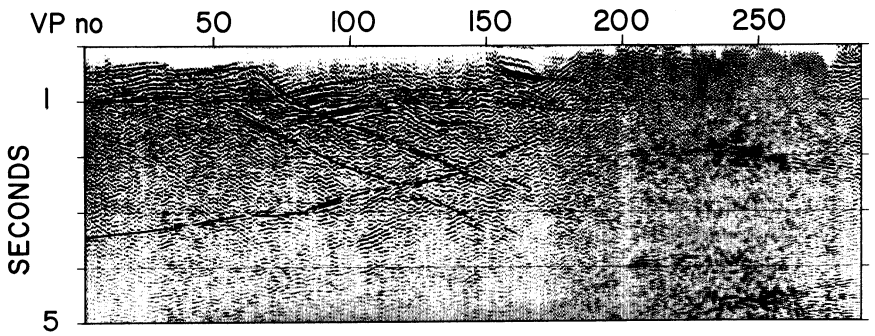

Fig. 11a. Normal incidence seismic image of the model in Figure 10a superimposed on the seismic data shown unmarked in Figure 2a. Offsets observed along H must be due to velocity effects.

sections which corresponds to a major change in surface geology (Figure 1). Visual inspection of correlated field files from line 1 indicates that there is little lateral change in seismic character within a given recording for any individual shot: however, the overall appearance of the records varies dramatically depending on the location of the vibrators (Figure 13a). Records corresponding to sources within or at the edge of the rift basin are very different in character from records corresponding to shot points east of the Montosa fault. VPs 188-202 lie on Precambrian outcrop at Abo Pass. West of VP 179, at least 6 m of Pleistocene pediment gravel cover the Cenozoic basin fill. Precambrian basement is covered to the east by gently dipping Pennsylvanian strata. VPs 179-188 are located on an alluvial fan covering the Los Pinos fault. The shot point gather from VP 197 (Figure 13a) is typical of recordings with sources within the rift basin. For these recordings, most of the seismic energy lies between 15 and 20 Hz (Figure 13). The high-frequency part of the sweep is essentially not transmitted into the ground. The shot point gather from VP 198 (Figure 13a), whose source is east of the Montosa fault, exhibits a spectrum richer in high frequencies with an average energy about 14 dB higher than for VP 197. It is important to note that these changes correspond to source location, not receiver location. For example, the receivers in Figure 13a straddle the fault zone yet show no significant change in seismic character within the record. This source-location dependent behavior can only be explained by a coupling phenomena.

Nonlinear effects (distortion) can occur depending upon whether a vibrator is resting on relatively consolidated or unconsolidated material [Edelmann, 1982]. Overdriving a vibrator against a "hard" surface can increase generation of harmonics, thus enriching the high end of the spectrum. The relative amount of energy input into the earth also depends upon the material properties of the ground upon which the vibrators are operating [Edelman, 1982]. Nowhere along the COCORP Abo Pass survey could we observe such a drastic change and correlate it with different receiver locations. Thus primary differences between shot point gathers are attributed to source location alone.

In general, the higher frequencies appear either not to have been generated in or transmitted through the basin fill. In the rift basin, Figure 13b shows an attenuation of 30 dB within less than two octaves, after only 2 s of two-way travel time. Power spectra calculated over time windows corresponding to increasing depths do not indicate any substantial additional attenuation below 2 s (approximately 4 km). Thus the gross seismic character along line 1 is fully established by 2 s travel time, which confirms that near-surface effects are primarily if not totally responsible for lateral variations in the gross appearance of the seismic section.

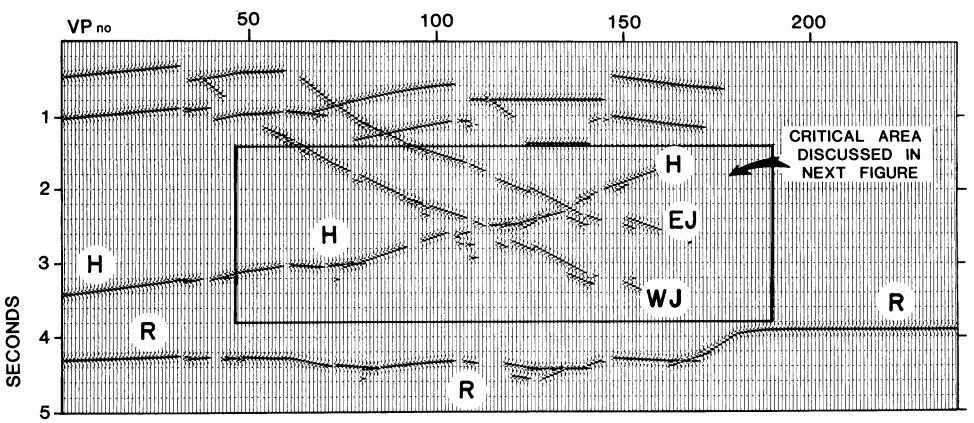

Fig. 11b. Same sythetics as above; note the magnitude of velocity pull-down effects on the horizontal reference interface R.

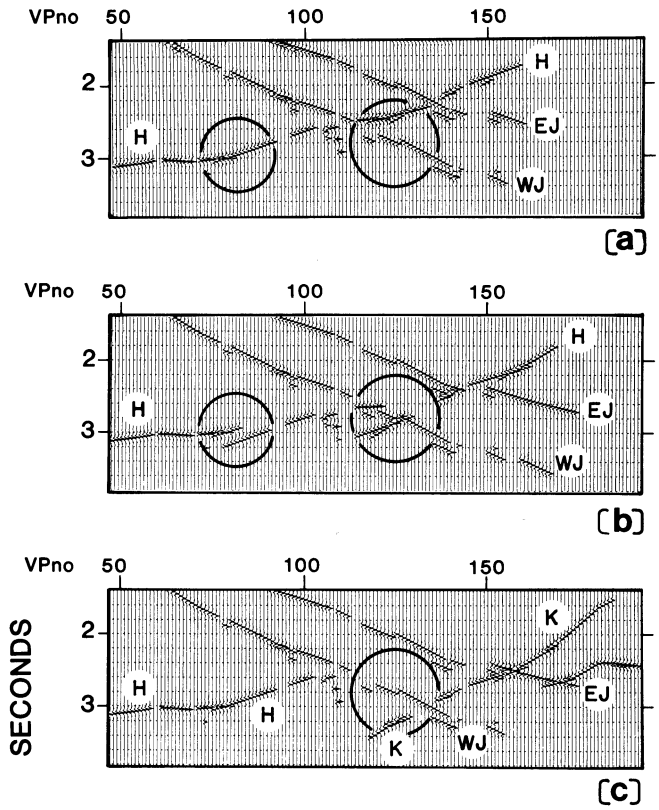

Fig. 12. Detail of synthetics; synthetics in Figures 12a, 12b and 12c correspond to the models postulated in Figures 10a, 10b, and 10c, respectively. Critical differences among the synthetics are circled. (a) Best fit. (b) Here, the offsets observed across H are larger than those observed on the actual data, suggesting that H is not offset by as much as the shallow sedimentary sequence, if at all. (c) Does not match the seismic data below VPs 110-140.

Amplitude decay curves were calculated from unstacked data at various locations along line 1 (Figure 13c). Recorded seismic energy can be considered as the sum of three terms: reflected signal (S), source-generated noise (N_s), and ambient noise (N_a). S and N_s both decay with time, whereas N_a has essentially a constant power during the time scale of a given shot. Although seismic energy recorded east of the rift boundary may not quite decay to ambient level within the first 20 s, energy decay curves from the basin to the west show a sharp decrease in amplitude during the first 4 s and are virtually flat after 10 or 12 s (Figure 13c). This observation suggests that source generated energy propagates much further beneath the flank of the rift basin, whereas it is not generated in or transmitted through the graben fill. Thus amplitude decay curves are consistent with the inference that signal-to-noise ratio of the data is much deteriorated below the basin when compared with traces shot east of the Paloma-Montosa fault zone.

Below and slightly west of the surface position of the Los Pinos fault is a deeply penetrating, near-vertical zone apparently devoid of continuous reflections (B, Figure 2). Brown et al. [1980] speculated that this zone might represent a major high angle fault zone (Los Pinos fault?) or a vertical intrusion at depth, while cautioning that it may also be an artifact of processing data which span such a large contrast in geology. The dramatic contrast in reflection strength and amplitude documented above is probably not a major factor in defining this zone, since the zone is imaged primarily by data collected from shot points uniformly west of the Los Pinos fault. However, ray path distortion within a CMP gather will smear reflections from portions of structures underlying a large lateral contrast in seismic velocities (such as across the Los Pinos fault), leading to a degraded stacked section [Peddy et al., 1986]. Since the signal-to-noise ratio of most of the individual field records is fairly high, a viable alternative to sophisticated processing such as ray path statics is the generation of stacked sections which include only a limited range of the data, thus limiting CMP smearing by reducing the fold. Indeed, though a "blank zone" is quite prominent on previously published sections [e.g., Brown et al., 1980], and also somewhat on Figure 2 (zone B), this is not the case on the near-range stack of Figure 9, despite the marked change in seismic character across the rift boundary. The segmented appearance of some weak events across zone B (e.g., S, Figure 9) is consistent with raypath

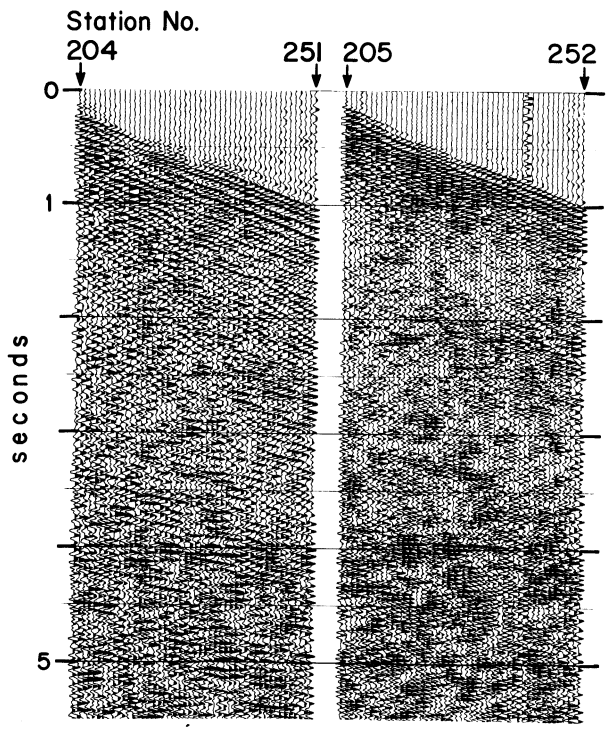

Fig. 13a. Example of two records from subsequent vibrator points, only 100 m apart; near offset is 600 m; receivers spacing is 100 m. Note the striking overall difference in character and frequency content that is quantitatively illustrated by the average power spectra plotted below the corresponding records; these spectra were calculated between 0 and 6 s.

distortion and velocity pull-down effects illustrated above by synthetic modeling. Thus our analysis indicates that the blank zone B is most likely an imaging artifact, although this does not rule out the presence of an intrusion or a structural dislocation at depth, such as a strike-slip boundary.

Discussion

Low-Angle Extensional Faulting at Depth Below the Albuquerque Basin

An increasing number of studies have identified large-scale low-angle normal faults or detachments in the Basin and Range province [e.g., Allmendinger et al., 1983]. Above such extensional features, faulted blocks are shown to have various degrees of tilt and can be bounded by both listric and planar normal faults [Wernicke and Burchfiel, 1982]. With the exception of the Jeter fault, low-angle normal faults have not yet been recognized from surface geology in the Albuquerque basin [Chamberlin et al., 1983].

Extension of the Hubell bench is interpreted to occur along fairly planar or only slightly listric Cenozoic normal faults which sole into or are truncated by a northwest dipping master fault (Figure 10a). This fault may be the Los Pinos fault or a reactivated Paloma-Montosa thrust. Its apparent dip on line 1 increases from 10° to 20° between VPs 10 and 150 (H, Figure 2). Assuming a constant strike of N49°E as determined above at VP 80, these apparent dips give true dips of 18° and 38°, respectively, indicating that H is fairly listric. However, if H corresponds to the Los Pinos fault, its strike at VP 150 should be close to N30°E (Figure 1), yielding a true dip of only 27° below VP 150. Whether this fault continues westward and underlies the whole southern Albuquerque basin is unclear, the quality of the COCORP data to the west being too poor to resolve this question.

Whereas the eastern rift boundary is associated with uplifts and major faults, structures on the west side of the basin are more subdued. The bordering uplifts are lower and more irregular,

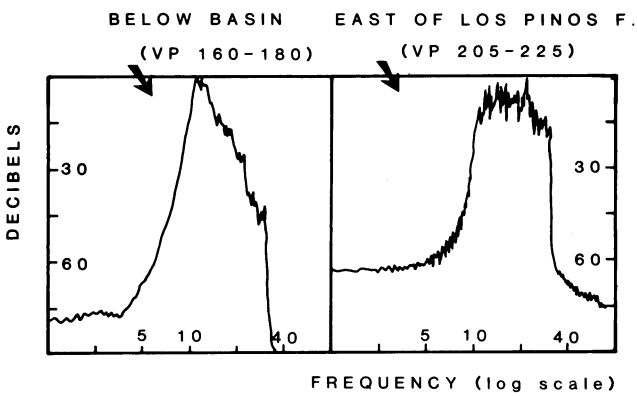

Fig. 13b. Average power spectra below and outside the rift basin, computed for times greater than 2 s (approximately 4 km); both plots are scaled relative to their respective maximum value.

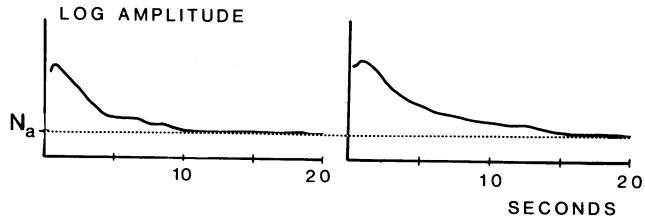

Fig. 13c. Average amplitude versus time decay curves were computed from unstacked traces, after muting of the refracted arrivals and applying normal move out corrections; the value at which the curves flatten is taken as an estimate of the ambient noise; the curve to the left corresponds to VPs 160-180 (i.e., below the rift basin) and shows a rapid decay of the energy in the top 4 s, the curve being virtually flat after 10 or 12 s; the curve to the right corresponds to VPs 205-225, located east of the rift basin; here, source generated energy propagates much further as indicated by the slower decay of the amplitude which does not quite reach ambient level within 20 s.

with little or no faulting at their margins [Kelley, 1979]. Detailed gravity data in the Albuquerque basin reflect the pronounced east-west asymmetry of the rift [Birch, 1982]. Gentle gravity gradients to the west contrast with large and steep gravity gradients along the eastern rift boundary. Modeling indicates that flexures rather than faults fit the data along portions of the western edge of the basin [Birch, 1982]. The large gravity gradients which mark the eastern rift boundary might be interpreted as the result of steeply dipping normal faults, but that is not consistent with recent studies of gravity and well data [Birch, 1982]. Cape et al. [1983] modeled the borders with listric faults. A low-angle, ramplike, buried master fault is also compatible with the gravity data to the east [Cordell, 1979].

Recent studies conclude that crustal scale flexure and uplift of the footwall are major features associated with normal faulting [Zandt and Owens, 1980; Jackson and MacKenzie, 1983]. The footwall is isostatically uplifted as a result of unloading by normal faulting. Thus the present interpretation of a major west dipping normal fault is consistent with the pronounced topographic asymmetry of the Albuquerque basin.

Reactivation of Preexisting Structures

In a crude sense, both Pennsylvanian and Laramide structures, as well as the more recent rift, appear to follow Precambrian trends defined from gravity and aeromagnetic data [Cordell, 1978]. The prominent northwesterly and northeasterly fault directions follow regional basement fabrics defined by aeromagnetic and gravity data [Cordell, 1976], suggesting that the Cenozoic trends may be inherited from Paleozoic or Precambrian structures. Structural and stratigraphic evidence for major pre-Miocene deformation along the basins that now form the RGR is reviewed by Chapin and Seager [1975] and Chapin and Cather [1981]. Tweto [1979] suggests that in

Colorado, the RGR follows westerly Precambrian structural trends. Baars [1982] used the Pennsylvanian strata as diagnostic evidence that the rift may have had a history going back to Precambrian times. However, there are also some differences between Laramide and Cenozoic trends, indicating that maybe only portions of the RGR are following preexisting structures or zones of weakness wherever these are appropriately located [e.g., Reed 1983].

In various places, the recognition of spatial relations between Cenozoic structures and Mesozoic or older structures or zones of weakness indicates that preexisting structural fabrics are likely to influence or even control any subsequent deformation of the continental crust, but the question of reactivation of a specific fault is difficult to assess [Allmendinger et al., 1982, 1986]. Some low-angle normal faults in the Basin and Range province are probably reactivated thrusts [Royse et al., 1975]. However, in other cases there is no conclusive evidence for reactivation of older structures. For example, detailed palinspastic reconstructions of the Sevier Desert detachment, based on deep seismic reflection data and all geological data available, indicate that it might be either mostly, if not entirely, a new Cenozoic normal fault [Sharp, 1984] or a reactivated Mesozoic thrust, both alternatives appearing equally plausible at the moment [Allmendinger et al., 1986]. In the Mormon mountains of southern Nevada, Miocene normal faults appear to truncate Mesozoic thrusts, and Wernicke [1981] concludes that preexisting thrust faults need not control the geometry of low-angle normal faults.

At the surface, the Los Pinos fault closely follows, and possibly locally joins, the Paloma and Montosa thrusts [Kelley, 1977, p. 44]. The possibility that the Cenozoic Los Pinos fault may converge at depth toward these Laramide thrusts is consistent with the COCORP data, though equivocal. Just north of the Albuquerque basin, a similar spatial relationship has been suggested between the Laramide thrust and the Neogene normal fault that bounds the Sangre de Cristo uplift [Sales, 1983], though low-angle normal faulting at depth is not documented along the San Luis basin. Sales interprets the postcompressional normal fault as a large gravity fault along which the uplift is downdropped toward the root zone of the thrusts that raised the uplift. The low-angle Cenozoic normal fault inferred to bound the southeastern Albuquerque basin projects to the surface in the vicinity of the Paloma-Montosa fault zone, suggesting possible reactivation of these Laramide structures. However, the strike of the Cenozoic master fault beneath the Hubell bench is significantly different (N49°E) from the average trend (N20°E) of the Laramide uplifts on the east side of the basin.

Basement Stratigraphy

To the east of the rift boundary, between 1.0 and 12 s on line 1, the Precambrian basement is characterized by a high density of strong, continuous events of varying dips. On Figure 2a, those reflections appear as bright as events attributed to the Socorro magma body (G, Figure 2b [Brown et al., 1980]). As discussed earlier, the signal-to-noise ratio of the data is much higher outside the graben. Average seismic amplitudes on the eastern end of line 1 are about 14 dB higher than beneath the basin, possibly contributing to the impression of strong reflections. Also, the strong S wave reflector discovered and interpreted as evidence for magma by Sanford et al. [1973] and mapped by various seismic methods does not extend east of VP 40 of line 1 [Rinehart et al., 1979; Brocher, 1981b]. The relatively high seismic amplitudes observed to the east are therefore not attributed to the presence of magma. Constructive interferences due to fine layering may contribute to the high reflectivity of the crust outside the rift.

Although the nature of the impressive layering of the basement to the east is uncertain, some inferences can be made from the extensive Precambrian outcrops that emerge from the Cenozoic graben fill. At least 1.4 km of Sevilleta rhyolite lies on top of a 2.2-km-thick series of quartzite and schist in the Los Pinos-Manzano mountains area [Muehlberger et al., 1967]. These metavolcanic and metasedimentary rocks have been intruded by granitic plutons of various sizes during at least two episodes of magmatism, 1570 and 1350 Ma. Transposed layering and low-angle faults have been inferred in the Precambrian rocks [Callender, 1983].

The Manzano-Los Pinos mountains as well as most of New Mexico belong to the 1650-1720 Ma Proterozoic province defined by Condie [1982]. Possibly being part of the same terrane, the basement imaged on the eastern end of line 1 may be similar to the basement imaged in the Hardeman County (Texas) and Oklahoma COCORP surveys [Brewer et al., 1981]. In particular, the strong 3-4 cycle event labeled P (Figure 2) may be compared to the layering observed on the southern Oklahoma lines (horizons A and B of Brewer et al. [1981]).

Conclusions

A dramatic lateral change in seismic character is conspicuous across the eastern rift margin. Major differences in amplitude and frequency content of the data correlate with source location alone and not with receiver location suggesting that variations in source coupling associated with surfacial geology is mainly, if not totally, responsible. Complex ray paths and anelastic attenuation by the graben fill may also contribute to the much deteriorated signal below the rift basin. A near-vertical zone, apparently devoid of continuous reflections, that seems to bound the eastern side of the basin is most likely an artifact of processing data which span the large lateral contrast in shallow seismic velocities across the Los Pinos fault. Neither a deep intrusion nor a near-vertical structure is required to explain this blank zone.

In spite of this imaging unevenness, reprocessing and synthetic seismic modeling of line 1 shed new light on the geometrical relationship between basement structures and shallow Cenozoic normal faults. Three-dimensional geometric analysis of the COCORP data indicates that the Joyita faults may be planar or slightly listric, but do not flatten with depth as dramatically as suggested by Cape et al. [1983]. Synthetic seismic sections indicate that the shallow normal faults do not offset an underlying northwesterly dipping horizon. This horizon, traced to a depth of at least 10 km, is interpreted as a Cenozoic

master fault bounding the southeastern side of the Albuquerque basin. This fault may be a new Cenozoic feature or a Laramide thrust, reactivated at depth during Cenozoic extension.

Acknowledgments. We are grateful to all of the individuals who contributed comments, ideas, and encouragements. Discussions with T. Hauge, L. Serpa, B. Payne, and C. Cape have been particularly helpful. We thank Conoco for giving us a copy of their reprocessed sections of the COCORP Socorro and Abo Pass profiles. L. Angell and J. Phoenix helped with the figures. We thank J. K. Costain and S. B. Smithson for their thorough reviews. The COCORP project is supported by National Science Foundation grants EAR82-12445 and EAR83-13569. B. de Voogd received partial funding in the form of a scholarship of the Society of Exploration Geophysicists Foundation. The data were recorded by Petty-Ray Geophysical Division of Geosource, Inc. and reprocessed on the MEGASEIS system (T.M. Seiscom Delta United, Inc.) at Cornell University. The synthetic seismic sections were calculated on the MEGASEIS using the Advanced Interpretive Modeling System (AIMS, T.M. Geoquest International). Department of Geological Sciences, Cornell University, contribution 819.

References

Al-Chalabi, M., An analysis of stacking, RMS, average, and interval velocities over a horizontally layered ground, Geophys. Prospect., 22, 458-475, 1974.

Allmendinger, R. W., J. A. Brewer, L. D. Brown, S. Kaufman, J. E. Oliver, and R. S. Houston, COCORP profiling across the Rocky Mountain front in southern Wyoming, 2; Precambrian basement structure and its influence on Laramide deformation, Geol. Soc. Am. Bull., 93, 1253-1263, 1982.

Allmendinger, R. W., J. Sharp, D. Von Tish, L. Serpa, L. Brown, S. Kaufman, J. Oliver, and R. B. Smith, Cenozoic and Mesozoic structure of the eastern Basin and Range from COCORP seismic reflection data, Geology, 11, 532-536, 1983.

Allmendinger, R. W., H. Farmer, E. Hauser, J. Sharp, D. Von Tish, J. Oliver, and S. Kaufman, Phanerozoic tectonics of the Basin and Range-Colorado Plateau transition from COCORP data and geologic data: A review, in Reflection Seismology: The Continental Crust, Geodyn. Ser., vol. 14, edited by M. Barazangi and L. Brown, pp. 257-268, AGU, Washington, D. C., 1986.

Baars, D. L., Paleozoic history of the Albuquerque trough: Implications of basement control on the Rio Grande rift, Field Conf. Guideb. N.M. Geol. Soc., 33rd, 153-157, 1982.

Birch, F. S., Gravity models of the Albuquerque basin, Rio Grande rift, New Mexico, Geophysics, 47, 1185-1197, 1982.

Brewer, J. A., L. D. Brown, D. Steiner, J. E. Oliver, S. Kaufman, and R. E. Denison, A Proterozoic basin in the southern midcontinent of the United States revealed by COCORP deep seismic reflection profiling, Geology, 9, 569-575, 1981.

Brocher, T. M., Shallow velocity structure of the Rio Grande rift north of Socorro, New Mexico: A reinterpretation, J. Geophys. Res., 86, 4960-4970, 1981a.

Brocher, T. M., Geometry and physical properties of the Socorro, New Mexico, magma bodies, J. Geophys. Res., 86, 9420-9432, 1981b.

Brown, L. D., P. A. Krumhansl, C. E. Chapin, A. R. Sanford, F. A. Cook, S. Kaufman, J. E. Oliver, and F. S. Schilt, COCORP seismic reflection studies of the Rio Grande rift, in Rio Grande Rift: Tectonics and Magmatism, edited by R. E. Riecker, pp. 169-184, AGU, Washington, D. C., 1979.

Brown, L. D., C. E. Chapin, A. R. Sanford, S. Kaufman, and J. Oliver, Deep structure of the Rio Grande Rift from seismic reflection profiling, J. Geophys. Res., 85, 4773-4800, 1980.

Callender, J., Transposition structures in Precambrian rocks of New Mexico, Field Conf. Guideb. N. M. Geol. Soc., 34th, 143-146, 1983.

Cape, C. D., S. McGeary, and G. A. Thompson, Cenozoic normal faulting and the shallow structure of the Rio Grande rift near Socorro, New Mexico, Geol. Soc. Am. Bull., 94, 3-14, 1983.

Chamberlin, R. M., Cenozoic domino-style crustal extension in the Lemitar Mountains, New Mexico, A summary, Field Conf. Guideb. N. M. Geol. Soc., 34th, 111-118, 1983.

Chamberlin, R. M., G. R. Osburn, C. E. Chapin, M. N. Machette, J. M. Barker, J. W. Hawley, S. M. Cather, J. C. Osburn, and O. J. Anderson, Field Conf. Guideb. N. M. Geol. Soc., 34th, 29-59, 1983.

Chapin, C. E., Evolution of the Rio Grande rift, in Rio Grande Rift: Tectonics and Magmatism, edited by R. E. Riecker, pp. 1-5, AGU, Washington, D. C., 1979.

Chapin, C. E., and S. M. Cather, Eocene tectonics and sedimentation in the Colorado plateau-Rocky Mountain area; Ariz. Geol. Soc. Dig., 14, 173-198, 1981.

Chapin, C. E., and W. R. Seager, Evolution of the Rio Grande rift in the Socorro and Las Cruces areas, Field Conf. Guideb. N. M. Geol. Soc., 26, 297-321, 1975.

Condie, K. C., Plate-tectonics model for Proterozoic continental accretion in the southwestern U.S., Geology, 10, 37-42, 1982.

Cordell, L., Aeromagnetic and Gravity Studies of the Rio Grande Graben in New Mexico between Belen and Pilar, Spec. Publ., N. M. Geol. Soc. 6, 62-70, 1976.

Cordell, L., Regional geophysical setting of the Rio Grande rift, Geol. Soc. Am. Bull., 89, 1073-1090, 1978.

Cordell, L., Sedimentary facies and gravity anomaly across master faults of the Rio Grande rift in New Mexico, Geology, 7, 201-205, 1979.

Edelmann, H. A. K., A contribution to the investigation of amplitude characteristics of vibrator signals, Geophys. Prospect., 30, 774-785, 1982.

Foster, R. W., Selected data for deep drill holes along Rio Grande rift in New Mexico, Circ. N. M. Bur. Mines Miner. Resour., 163, 236-237, 1978.

Fountain, D. M., C. A. Hurich, and S. B. Smithson, Seismic reflectivity of mylonite zones in the crust, Geology, 12, 195-198, 1984.

Hale, D., Dip-moveout by Fourier transform, Geophysics, 49, 741-757, 1984.

Jackson, J., and D. McKenzie, The geometrical evolution of normal fault systems, J. Struct. Geol., 5, 471-482, 1983.

Jurdy, D. M., and T. M. Brocher, Shallow velocity structure of the Rio Grande rift near Socorro, New Mexico, Geology, 8, 185-189, 1980.

Kelley, V. C., Geology of Albuquerque Basin, New Mexico, Mem. N. M. Bur. Mines Miner. Resour., 33, 60 pp., 1977.

Kelley, V. C., Tectonics, middle Rio Grande Rift, New Mexico, in Rio Grande Rift: Tectonics and Magmatism, edited by R. E. Riecker, pp. 57-70, AGU, Washington, D. C., 1979.

Larner, K. L., L. Hatton, B. S. Gibson, and I.-C. Hsu, Depth migration of imaged time sections, Geophysics, 46, 734-750, 1981.

Machette, M. N. (Compiler), Preliminary geologic map of the Socorro 1°x 2° quadrangle, central New Mexico, U.S. Geol. Surv. Open File Rep., 78-607, 1978.

Machette, M. N., Quaternary and Pliocene faults in the La Jencia and southern part of the Albuquerque-Belen basins, New Mexico: Evidence of fault history from fault-scarp morphology and quaternary geology, Field Conf. Guideb. N. M. Geol. Soc., 33rd, 161-169, 1982.

Machette, M. N., and R. G. McGimsey, Quaternary and Pliocene faults in the Socorro and western part of the Fort Sumner 1°x2° quadrangles, New Mexico, U.S. Geol. Surv. Misc. Field Stud. Map, MF-1465-A, 1983.

Muehlberger, W. R., R. E. Denison, and E. G. Lidiak, Basement rocks in continental interior of United States, Am. Assoc. Pet. Geol. Bull., 51, 2351-2380, 1967.

Myers, D. A., Geologic map of the Scholle quadrangle, Socorro, Valencia, and Torrance counties, New Mexico, quadrangle map, U.S. Geol. Surv., Denver, CO., 1977.

Myers, D.A., E.J. McKay, and J.A. Sharps, Geologic map of the Becker Quadrangle, Valencia and Socorro counties, New Mexico, quadrangle map, U.S. Geol. Surv., Denver, CO., 1981.

Oliver, J., and S. Kaufman, Profiling the Rio Grande rift, Geotimes, 21, 20-23, 1976.

Olsen, K. H., G. R. Keller, and J. N. Stewart, Crustal Structure along the Rio Grande rift from seismic refraction profiles, in Rio Grande Rift: Tectonics and Magmatism, edited by R. E. Riecker, pp. 127-143, AGU, Washington, D. C., 1979.

Peddy, C., L. Brown, and S. Klemperer, Interpreting the deep structure of rifts with synthetic seismic sections, in Reflection Seismology: A Global Perspective, Geodyn.Ser. vol. 13, edited by M. Barazangi and L. Brown, AGU, Washington, D. C., 1986.

Ragan, D. M., Structural Geology: An Introduction to Geometrical Techniques, 2nd ed., 208 pp., John Wiley, New York, 1973.

Reed, J. C., Jr., Precambrian rocks near the intersection of the Jemez zone and Rio Grande rift, New Mexico, paper presented at the Geological Society of America meeting, Salt Lake City, Utah, 1983.

Reiche, P., Geology of the Manzanita and north Manzano Mountains, New Mexico, Geol. Soc. Am. Bull., 60, 1183-1212, 1949.

Rinehart, E. J., A. R. Sanford, and R. M. Ward, Geographic extent and shape of an extensive magma body at midcrustal depths in the Rio Grande rift area near Socorro, New Mexico, in Rio Grande Rift: Tectonics and Magmatism, edited by R. E. Riecker, pp. 127-143, AGU, Washington, D. C., 1979.

Royse, F., M. A. Warner, and D. L. Reese, Thrust belt structural geometry and related stratigraphic problems Wyoming-Idaho-northern Utah, in Symposium on Deep Drilling Frontiers in the Central Rocky Moutains, edited by D. W. Bolyard, pp. 41-54, Rocky Mountain Association of Geologist, Denver, Colo., 1975.

Sales, J. K., Collapse of Rocky Mountain basement uplifts, pp. 79-97, Rocky Mountain Association of Geologists, 1983.

Sanford, A. R., O. S. Alptekin, and T. R. Toppozada, Use of reflection phases on microearthquake seismograms to map an unusual discontinuity beneath the Rio Grande rift, Bull. Seismol. Soc. Am., 63, 2021-2034, 1973.

Sharp, J. W., West-central Utah: Palinspastically restored sections constrained by COCORP seismic reflection data, M.S. thesis, Cornell Univ., Ithaca, N. Y., 1984.

Smithson, S. B, J.A. Brewer, S. Kaufman, J.E. Oliver, and C.A. Hurich, Structure of the Laramide Wind River uplift, Wyoming, from COCORP deep reflection data and from gravity data, J. Geophys. Res., 84, 5955-5972, 1979.

Stark, J. T., Geology of the South Manzano Mountains, New Mexico, Bull. N. M. Bur. Mines Miner. Resour., 34, 49 pp., 1956.

Stark, J. T., and E. C. Dapples, Geology of the Los Pinos Mountains, New Mexico, Geol. Soc. Am. Bull., 57, 1121-1172, 1946.

Toppozada, T. R., and A. R. Sanford, Crustal structure in central New Mexico interpreted from the Gasbuggy explosion, Bull. Seismol. Soc. Am., 66, 877-886, 1976.

Tweto, O., The Rio Grande Rift system in Colorado, in Rio Grande Rift: Tectonics and Magmatism, edited by R. E. Riecker, pp. 33-56, AGU, Washington, D. C., 1979.

Wernicke, B., Low-angle normal faults in the Basin and Range province: Nappe tectonics in an extending orogen, Nature, 291, 645-648, 1981.

Wernicke, B., and B. C. Burchfiel, Modes of extensional tectonics, J. Struct. Geol., 4, 105-115, 1982.

Woodward, L. A., Rate of crustal extension across the Rio Grande rift near Albuquerque, New Mexico, Geology, 5, 269-272, 1977.

Zandt, G., and T. J. Owens, Crustal flexure associated with normal faulting and implications for seismicity along the Wasatch front, Utah, Bull. Seismol. Soc. Am,. 70, 1501-1520, 1980.

B. de Voogd, L.D. Brown and C. Merey, Institute for the Study of the Continents, Snee Hall, Cornell University, Ithaca, NY 14853.

(Received March 4, 1985;
revised December 23, 1985;
accepted January 8, 1986.)